ARTICLE

High-throughput screening campaigns against a PI3Kα isoform bearing the H1047R mutation identified potential inhibitors with novel scaffolds

Jia Wang[1], Grace Qun Gong[1,2,3], Yan Zhou[1], Woo-Jeong Lee[2], Christina Maree Buchanan[2,3], William Alexander Denny[3,4], Gordon William Rewcastle[3,4], Jackie Diane Kendall[4], James Michael Jeremy Dickson[3,5], Jack Urquhart Flanagan[3,4], Peter Robin Shepherd[2,3], De-Hua Yang[1] and Ming-Wei Wang[1,6]

The phosphatidylinositol 3-kinase (PI3K) pathway is involved in many cellular functions including cell growth, metabolism, and transformation. Hyperactivation of this pathway contributes to tumorigenesis, therefore, PI3K is a major target for anticancer drug discovery. Since the PI3Kα isoform is implicated mostly in cancer, we conducted a high-throughput screening (HTS) campaign using a 3-step PI3K homogenous time-resolved fluorescence assay against this isoform bearing the H1047R mutation. A total of 288,000 synthetic and natural product-derived compounds were screened and of which, we identified 124 initial hits that were further selected by considering the predicted binding mode, relationship to known pan-assay interference compounds and previous descriptions as a lipid kinase inhibitor. A total of 24 compounds were then tested for concentration-dependent responses. These hit compounds provide novel scaffolds that can potentially be optimized to create novel PI3K inhibitors.

Keywords: high throughput screening; PI3 kinase; PI3Kα H1047R; inhibitors; molecular modeling.

INTRODUCTION
The phosphatidylinositol 3-kinase (PI3K) family of lipid kinases catalyzes the phosphorylation of 3-OH groups on the inositol ring of phosphatidylinositols embedded within membrane phospho-lipids [1]. PI3Ks can be divided into three different classes based on structural similarity, mechanism of activation, and substrate specificities [2, 3]. Class I PI3Ks catalyze the conversion of phosphatidylinositol 4,5-bisphosphate (PIP_2) to phosphatidylino-sitol 3,4,5-trisphosphate (PIP_3) [4]. PIP_3 then acts as a secondary messenger to recruit and activate downstream signaling proteins to control important cellular processes including growth, meta-bolism, and migration [5, 6].

Among the class I PI3Ks, the PI3Kα isoform, a heterodimer consisting of a p110α catalytic subunit encoded by *PIK3CA* and a p85α regulatory subunit encoded by *PIK3R1*, is implicated mostly in cancer [7–9]. The p110α catalytic subunit consists of five domains: an N-terminal adapter-binding domain that interacts with the regulatory subunit, a Ras-binding domain that mediates the interaction of p110 and Ras, a C2 domain that is involved in lipid binding, a helical domain that acts as a scaffold for other domains, and a C-terminal kinase domain where the ATP-binding and PIP_2-binding sites are located [10]. PI3Kα is activated upon binding of receptor tyrosine kinases at phosphorylated tyrosines

in YXXM motifs by SH2 domains in the p85α regulatory protein, relieving the inhibition of the p85α nSH2 domain on the p110α catalytic subunit [8]. PI3Kα is recruited to the lipid membrane upon activation, where it phosphorylates PIP_2 to PIP_3, causing an intracellular signaling cascade [11].

The *PIK3CA* gene is frequently mutated in many cancers, with the majority of mutations clustering in two hotspots [12]. One is located in the helical domain and involves the amino acid substitutions E542K and E545K (Catalog of somatic mutations in cancer, http://cancer.sanger.ac.uk). These mutations activate PI3Kα by mimicking and enhancing the growth factor-activated state and by relieving the inhibition imposed by the p85α nSH2 domain on the p110α subunit [13, 14]. The second hotspot is located in the kinase domain and involves substitutions of H1047 with R, L, or Y. These substitutions activate the enzyme by enhancing its membrane binding capability and increasing its access to PIP_2 [13, 15, 16]. These two hotspot activate the enzyme by different mechanisms and are synergistic in vitro [14, 17, 18]. However, the presence of both hotspot mutations has not yet been identified in the same tumor [9]. Both the E545K and the H1047R mutations are found in a range of cancer cell lines, such as breast, ovarian, prostate, and colon cancer [12, 19–21].

[1]The National Center for Drug Screening and the CAS Key Laboratory of Receptor Research, Shanghai Institute of Materia Medica, Chinese Academy of Sciences (CAS), Shanghai 201203, China; [2]Department of Molecular Medicine and Pathology, The University of Auckland, Auckland, New Zealand; [3]The Maurice Wilkins Centre, Auckland, New Zealand; [4]Auckland Cancer Society Research Centre, Auckland, New Zealand; [5]School of Biological Sciences, The University of Auckland, Auckland, New Zealand and [6]School of Pharmacy, Fudan University, Shanghai 201203, China
Correspondence: Ming-Wei Wang (mwwang@simm.ac.cn)
These authors contributed equally: Jia Wang, Grace Qun Gong, Yan Zhou

New inhibitor screening against a mutant PI3Kα
J Wang et al.

1817

Available crystal structures of PI3K from the Protein Data Bank (PDB) show that all known inhibitors interact with the ATP-binding site, which is located in a cleft between the N-terminal and C-terminal lobes of the kinase domain [9]. There are two regions in the cleft that are present in all isoforms: a hinge region located at the base of the ATP-binding cavity that provides a hydrogen bond donor and acceptor site through the backbone amide of a valine amino acid and a hydrophobic pocket termed the affinity pocket [22]. PI3Kα-selective inhibition can be achieved by interacting with the p110α-specific amino acid Gln859 in a non-conserved area called region I [21, 23–25].

To date, a number of selective PI3Kα inhibitors have been developed, including the clinical candidate alpelisib and its analogs [23, 26–28]; the PIK-75 series [29, 30]; the NVS-PI3-2 series, which was discovered via high-throughput screening (HTS) [31]; the GDC-0326 series [32]; and the CNX-1351 series [33]. However, none of these inhibitors are selective for the H1047R oncogenic mutant over wild-type PI3Kα. As overexpression and mutation of PI3Kα are associated with cancer, developing inhibitors that are selective for PI3Kα may be more beneficial than inhibiting all class I PI3Ks [34]. Furthermore, selectively targeting the oncogenic mutant may widen the therapeutic window and reduce adverse side effects commonly associated with PI3K inhibition including hyperglycemia [35, 36].

HTS is a method frequently used to discover hit compounds for drug development. Meanwhile, molecular docking has also become an essential tool often employed in drug discovery during the past few decades [37, 38]. Molecular docking is a computer-based method that can predict the conformation of small organic molecules in a target site on a protein of interest with a substantial degree of accuracy [39]. It can also be used as a screen to identify compounds within large libraries that best match the target site [37]. By using a combination of HTS and molecular docking, we aim to discover novel scaffolds for the development of PI3K inhibitors, and importantly, compounds that are potentially selective for H1047R mutant over wild-type PI3Kα.

MATERIAL AND METHODS

Protein expression and purification
PI3K proteins were expressed and purified as previously reported [24]. Briefly, recombinant baculovirus-containing coding sequences for the full-length wild-type or H1047R p110α catalytic subunit and p85α regulatory subunit were used to infect Sf9 cells (Life Technologies, Carlsbad, CA, USA). Cultured cells were then centrifuged at $666 \times g$, and the pellets were resuspended in 20 mM Tris, 137 mM NaCl, pH 8.0, flash frozen in liquid nitrogen and stored frozen at −20 °C. The frozen cell pellets were resuspended with gentle agitation in 25 mM Tris pH 8.0, 0.5% NP-40 alternative (Calbiochem, San Diego, CA, USA) and complete EDTA-free protease inhibitors (Roche, Basel, Switzerland) at room temperature until lysed as assessed by light microscopy. Cell lysates were centrifuged at $20,000 \times g$ for 30 min at 4 °C, the supernatant was removed and adjusted to 5% (v/v) glycerol, 150 mM NaCl, 7.5 mM imidazole, and 20 µg/mL RNAseA (Roche) and then passed through a 0.45 µm filter before loading onto a Talon-Co^{2+} resin column (Clontech, Mountain View, CA, USA) pre-equilibrated in 25 mM Tris pH 8.0, 100 mM NaCl, 5% (v/v) glycerol, and 7.5 mM imidazole. The resin was washed with ten column volumes of 25 mM Tris pH 8.0, 150 mM NaCl, 7.5 mM imidazole, and 5% glycerol. Protein was eluted from the column with 25 mM Tris pH 8.0, 150 mM NaCl, 150 mM imidazole, and 5% glycerol. Eluted protein was dialyzed overnight in 50 mM Tris pH 8.0, 100 mM NaCl, 1 mM DTT, and 5% glycerol at 4 °C. The dialyzed protein was centrifuged at $10,000 \times g$ for 10 min at 4 °C to remove precipitated material, and the supernatant was desalted to 40 mM NaCl using a Pharmacia Hi-trap desalting column (GE Healthcare; Little Chalfont, UK)

according to the manufacturer's instructions. The desalted protein was applied to a MonoQ column (GE Healthcare) pre-equilibrated in 50 mM Tris pH 8.0, 40 mM NaCl, 1 mM DTT, 5% glycerol and fractionated over a gradient from 40–200 mM NaCl in the same buffer.

Compound library
The compound library used in this study consisted of 288,000 synthetic and natural product-derived compounds solubilized in 100% DMSO prior to application in the HTS campaign. The structural diversity covered lactams, heterocycles, amides, secondary amides, sulfonates, sulfonamides, etc. One of the criteria for compound entry to this library is high purity (>95%). The collection is under strict quality control management. Both the purity and structures of randomly selected compounds were checked regularly (120 per month). Among the 8061 samples checked as of 27 April 2018, 99.06% showed correct structures according to the database information. The overall purity among them is 89.28%, which is sufficient for us to conduct HTS campaigns. This criterion applies to the 24 hits reported in this paper.

HTS campaign
HTS was carried out in black 384-well microtiter plates (PerkinElmer, Boston, MA, USA) using the 3-step PI3K homogenous time-resolved fluorescence (HTRF) assay (Millipore, Burlington, MA, USA) following the manufacturer's instructions. Wild-type and H1047R PI3Kα were titrated and used at a concentration equivalent to their EC_{65} values, and compounds were screened at a final concentration of 10 µM unless otherwise stated. Briefly, 0.5 µL of compounds were preincubated with 14.5 µL of enzyme and PIP_2 substrate for 10 min, before addition of 5 µL of ATP to achieve a final ATP concentration of 10 µM, similar to the Km of ATP as previously reported [40]. The total reaction volume was 20 µL, and the reaction was allowed to proceed for 45 min at room temperature before the addition of stop solution and detection mixture provided in the kit (Millipore). The plates were then incubated for 3 h in the dark and read using an EnVision Multilabel Plate Reader (PerkinElmer; 320/620/665). The experiment was done in duplicates. Hits identified from the primary screen using PI3Kα H1047R were subsequently rescreened against H1047R and counter-screened against wild-type PI3Kα at 10 µM.

Lipid kinase IC$_{50}$ determination
IC$_{50}$ values were determined using the HTRF assay described above. Selected hits were dissolved and serially diluted in 100% DMSO, with a final in-assay concentration of 2.5% DMSO. The results were obtained using an EnSpire Multimode Plate Reader (PerkinElmer; 320/620/665) and analyzed using GraphPad Prism 6 nonlinear regression (curve fit), log (inhibitor) vs. response variable slope (four parameters) with constraints added at 0 and 100.

Molecular modeling
Hits discovered from the HTS experiments were prepared for docking using SYBYLX2.1.1. The protonation state for pH 7.0 was generated using ProtoPlex, up to ten stereocenters were enumerated using StereoPlex, and the 3D models were generated using CONCORD with the CCR limit set at 0.4. Molecular docking was performed using GOLD v5.2.2 [41]. The human PI3Kα structure (PDB: 2RD0) was prepared for docking as described previously [42]. The docking site was defined as an 18 Å cavity centered on the CD1 atom of Ile800, and the docking was carried out with the ChemScore scoring function modified for use with kinases. All protein and ligand atom types were generated automatically within GOLD. Where possible, known ring conformations were used, otherwise the ligand flexibility terms were kept at default values. The diverse solutions option

was turned on and set to 2.0 Å, each ligand was docked five times using a search efficiency of 200%, and five poses were kept per ligand. All poses were then rescored using the ChemScore Kinase scoring function with the ligand minimization and receptor-depth scaling options turned on.

Statistical analysis

Results were analyzed using GraphPad Prism 6 and representatives of at least two independent experiments in duplicate or triplicate. Statistical significance was determined using multiple t-tests. $*P < 0.05$, $**P < 0.01$, $***P < 0.001$.

Z' value was evaluated by 192 enzyme control wells and 192 no-enzyme control wells before the HTS:

$$Z' = 1 - \frac{3 \times (\text{SDNEC} + \text{SDEC})}{|\text{MNEC} - \text{MEC}|}$$

MEC indicates the mean value of enzyme control wells. SDEC indicates the standard deviation of enzyme control wells. MNEC indicates the mean value of no-enzyme control wells. SDNEC indicates the standard deviation of no-enzyme control wells.

Inhibition (%) was calculated using the following equation:

$$\text{Inhibition } (\%) = \left(1 - \frac{\text{Signal}_{\text{test}} - \text{Signal}_{\text{NEC}}}{\text{Signal}_{\text{EC}} - \text{Signal}_{\text{NEC}}}\right) \times 100\%$$

$\text{Signal}_{\text{test}}$ indicates the value of each compound-test well. $\text{Signal}_{\text{NEC}}$ indicates the mean value of no-enzyme control wells. $\text{Signal}_{\text{EC}}$ indicates the mean value of enzyme control wells.

RESULTS AND DISCUSSION

High-throughput screening campaigns against PI3Kα

To identify new scaffolds and discover hit compounds that are active against the H1047R mutant, an HTS campaign was performed on the PI3Kα H1047R mutant. The HTS campaign included an initial screen of 288,000 compounds, followed by subsequent confirmation on H1047R, counter-screening of active hits against wild-type PI3Kα and IC$_{50}$ determination of selected hits in wild-type and H1047R PI3Kα. The 288,000 compounds were divided into three batches and screened against H1047R PI3Kα at 10 µM. The Z' value of the screening assay was 0.42 with a signal to background ratio (S/B ratio) of 3.11 and a coefficient of variation (CV) value of 11% (Fig. 1). The HTS results are summarized in Fig. 2. Batch 1 consisted of 80,000 compounds and gave 76 hits with
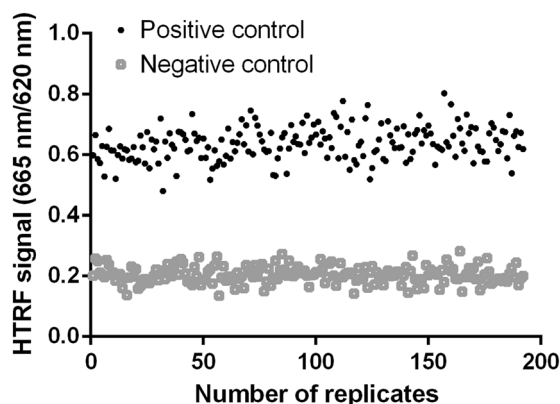

Fig. 1 Z' value and S/B ratio determination. The assay was performed under optimized conditions with H1047R PI3Kα. Negative control indicates the HTRF signal in the presence of enzyme in 2.5% DMSO. Positive control indicates the HTRF signal in the absence of enzyme in 2.5% DMSO. A total of 192 replicates were examined. The Z' value is 0.42, and the S/B ratio is 3.11
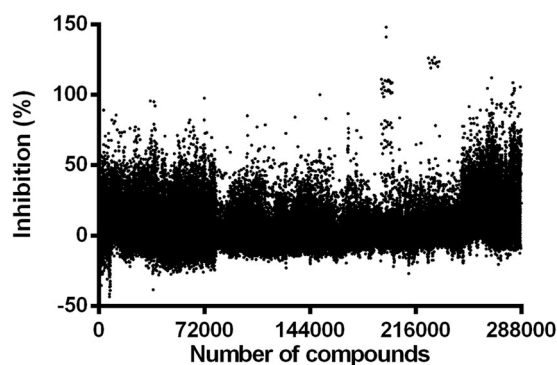

Fig. 2 HTS of 288,000 small molecule compounds using the 3-step PI3K HTRF assay. The results are expressed as the percentage of inhibition of each sample on PI3K catalytic activity using PIP$_2$ as the substrate

greater than 50% inhibition. For batches 2 and 3, the enzyme was less active than those used for batch 1, hence requiring more protein. To compensate for this and to increase the number of hit compounds, the cut-off for inhibition was lowered to 30%. These two combined batches consisted of 208,000 compounds and retrieved 112 hits with inhibition greater than 30%. Therefore, a total of 188 hits were identified from the HTS campaign. In the secondary screen, the 188 initial hits were rescreened against H1047R and then counter-screened at 10 µM against wild-type PI3Kα (Supplementary Figures 1–3). This approach yielded a total of 124 confirmed hits, and statistical analysis was carried out to determine whether they were selective for the H1047R mutant. The identified hits either had minimal selectivity for H1047R over wild-type after further testing in concentration response assays or were not further investigated due to unfavorable structures. Therefore, it seems that most of the confirmed hits were not selective for H1047R PI3Kα over wild-type PI3Kα, suggesting that it is difficult to achieve selectivity by probing the in vitro catalytic activity. This finding is in agreement with studies showing that the increase in activity of the H1047R mutant is not due to increased catalytic site activity but rather is due to increased membrane binding [15, 16, 43].

Identification of novel PI3Kα inhibitors

Although the HTS campaign did not yield hits that were selective for the H1047R mutant, the screen did discover some interesting structures. A major drawback in developing novel scaffolds is the undruggable nature of hit compounds; hence, the 188 initial hits were filtered for promiscuous compounds and non-drug-like groups. The pan-assay interference compounds (PAINS) substructure filter developed by Baell et al. [44] was used to remove compounds known to interfere with the assay through nonspecific mechanisms. An interpretation of this output is that any activity observed for the compounds that failed the PAINS filter might be related to mechanisms other than inhibiting the enzyme like a well-behaved reversible inhibitor. Of the 188 initial hits, only 102 compounds passed the PAINS filter, as implemented in SYBYLX2.1.1. They were also put through a filter for undesirable substructures that in general would not be found in drug-like molecules, which is also implemented in SYBYLX2.1.1. Of the 188 initial hits, 75 compounds passed the substructure filter, and only 53 compounds passed this and the PAINS filter.

Predicting a potential mechanism of inhibitory activity

Since the hits identified were active against both wild-type PI3Kα and the H1047R mutant enzyme, molecular docking was used to predict potential binding poses for the ligands in the PI3Kα active site. This approach was performed to find compounds that participate in interactions considered important for PI3Kα

New inhibitor screening against a mutant PI3Kα
J Wang et al.

1819

Table 1. IC$_{50}$ of active hits identified in the high-throughput screening (HTS) campaign

Compound	Structure	Chemical formula	Molecular Weight	IC$_{50}$ (µM)	
				H1047R	Wild-type
WNN0442-F002		C$_{10}$H$_{17}$N$_5$S	239.3	3.7	3.0
WNN0478-H007		C$_{22}$H$_{24}$O$_4$S	384.5	16.1	15.5
WNN0511-D006		C$_{14}$H$_{11}$FO$_5$	278.2	32.1	19.5
WNN0777-A004		C$_{22}$H$_{24}$O$_4$S	384.5	22.2	24.3
WNN0963-C010		C$_{14}$H$_{11}$ClO$_4$	278.7	115.3	55.5
WNN1237-B004		C$_{14}$H$_{11}$N$_3$O$_2$S	285.3	16.3	7.7
WNN1334-E008		C$_{16}$H$_8$Cl$_2$N$_2$O$_2$	331.2	34.2	23.2
WNN1489-B003		C$_{14}$H$_{10}$N$_4$S$_2$	298.4	12.9	11.7
WNN1541-G008		C$_{20}$H$_{20}$N$_2$O$_4$	352.4	8.1	7.1
WNN1560-A006		C$_{13}$H$_{18}$N$_2$O$_2$S	266.4	20.9	8.9

New inhibitor screening against a mutant PI3Kα
J Wang et al.

1820

Table 1 continued
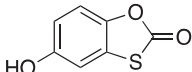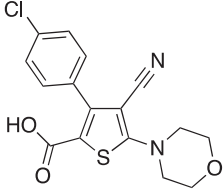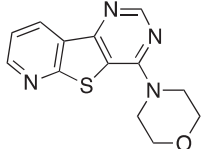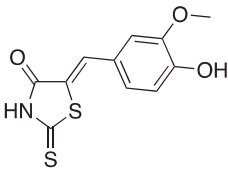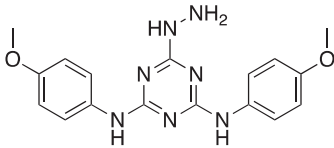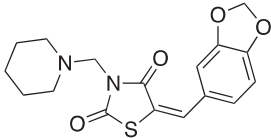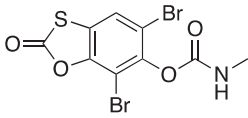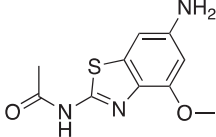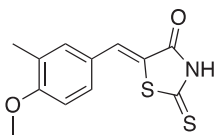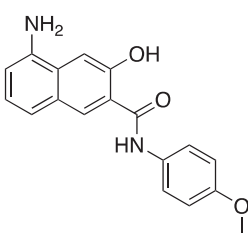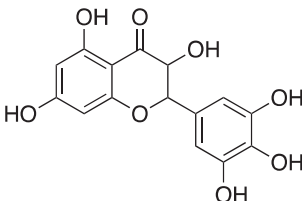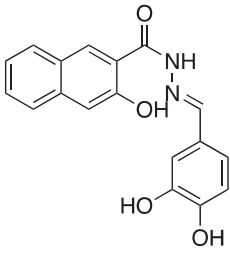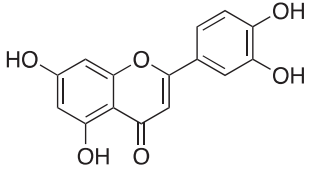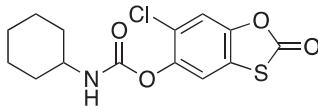
WNN0114-H009		$C_7H_4O_3S$	168.2	11.7	9.4
WNN0245-C009		$C_{16}H_{13}ClN_2O_3S$	348.8	29.4	28.3
WNN0429-D004		$C_{13}H_{12}N_4OS$	272.3	66.8	65.2
WNN0809-B004		$C_{11}H_9NO_3S_2$	267.3	7.8	6.8
WNN0829-H002		$C_{17}H_{19}N_7O_2$	353.4	47.0	34.9
WNN0901-F002		$C_{17}H_{18}N_2O_4S$	346.4	7.0	6.3
WNN1360-D011		$C_9H_5Br_2NO_4S$	383.0	3.1	2.7
WNN1414-G002		$C_{10}H_{11}N_3O_2S$	237.3	9.7	12.0
WNN2869-C007		$C_{12}H_{11}NO_2S_2$	265.4	2.1	2.0
WNN3162-F009		$C_{18}H_{16}N_2O_3$	308.3	124.6	84.2

New inhibitor screening against a mutant PI3Kα
J Wang et al.

1821

Table 1 continued

WNN4101-D008		$C_{15}H_{10}O_8$	318.2	2.5	2.4
WNN0671-D007		$C_{18}H_{14}N_2O_4$	322.3	2.2	2.6
WNN0471-H011		$C_{15}H_{10}O_6$	286.2	2.8	3.0
WNN0580-E008		$C_{14}H_{14}ClNO_4S$	327.8	5.9	5.0

inhibitors and to also identify compounds that potentially have novel mechanisms of action. All known PI3K inhibitors form hydrogen-bond interactions with the backbone amide of Val851 at the linker, and PI3Kα-selective inhibitors achieve their selectivity by interacting with the p110α-specific amino acid Gln859 [21, 23]. The five poses kept for each ligand were examined for a predicted hydrogen-bond interaction with the backbone amide of Val851 and the side chain carboxamide of Gln859 using the default hydrogen bond descriptor settings implemented in Hermes. Molecular docking data showed that of the 188 initial hits, 157 compounds were predicted to form hydrogen-bond interactions with the Val851 linker, and only three of these were also predicted to form a hydrogen bond with both polar groups of the Gln859 side chain as reported for PI3Kα-selective inhibitors [21, 23–25]. These docking results suggest that few of the active molecules are likely to be PI3Kα-selective, although the active compounds were not tested on other class I PI3K isoforms.

IC$_{50}$ determination of active hits
Based on the combination of biochemical data, predicted binding modes and chemical structure analysis, 24 compounds from the confirmed hits were prioritized for further investigation. IC$_{50}$ values were determined against both the wild-type and H1047R mutant enzymes. From these candidates, three compounds (WNN0429-D004, WNN1560-A006, and WNN4101-D008) have scaffolds similar to previously described PI3K inhibitors, and another two (WNN1237-B004 and WNN1489-B003) possess an embedded hydrogen bond donor–acceptor motif found in kinase inhibitors [45, 46]. This result demonstrates that the HTS protocol employed is capable of discovering lipid kinase inhibitors that block the ATP-binding site.

The results showed that most of the compounds have IC$_{50}$ values in the low micromolar range and that none of them were significantly more potent against the H1047R mutant enzyme than against the wild-type enzyme (Table 1). However, several novel structures were identified, and these may potentially act as starting points for future optimization to create potent PI3K inhibitors.

In summary, we presented the application of the PI3K homogenous time-resolved fluorescence assay to an HTS setting. In combination with molecular modeling, this approach led to the identification of hits with novel scaffolds, and our findings offer novel structures and promising tools for PI3K drug discovery.

AUTHOR CONTRIBUTION
PRS and MWW designed research. JW, GQG, YZ, WJL, CMB, JMJD, and JUF performed research. JW, GQG, YZ, WAD, GWR, JDK, JUF, DHY, PRS, and MWW analyzed data. GQG, CMB, JUF, and MWW wrote the paper.

New inhibitor screening against a mutant PI3Kα
J Wang et al.

1822

ADDITIONAL INFORMATION

The online version of this article (https://doi.org/10.1038/s41401-018-0057-z) contains supplementary material, which is available to authorized users.

REFERENCES

1. Williams R, Berndt A, Miller S, Hon WC, Zhang X. Form and flexibility in phosphoinositide 3-kinases. Biochem Soc Trans. 2009;37:615–26.
2. Asati V, Mahapatra DK, Bharti SK. PI3K/Akt/mTOR and Ras/Raf/MEK/ERK signaling pathways inhibitors as anticancer agents: Structural and pharmacological perspectives. Eur J Med Chem. 2016;109:314–41.
3. Katso R, Okkenhaug K, Ahmadi K, White S, Timms J, Waterfield MD. Cellular function of phosphoinositide 3-kinases: implications for development, homeostasis, and cancer. Annu Rev Cell Dev Biol. 2001;17:615–75.
4. Fruman DA, Meyers RE, Cantley LC. Phosphoinositide kinases. Annu Rev Biochem. 1998;67:481–507.
5. Engelman JA, Luo J, Cantley LC. The evolution of phosphatidylinositol 3-kinases as regulators of growth and metabolism. Nat Rev Genet. 2006;7: 606–19.
6. Vanhaesebroeck B, Leevers SJ, Panayotou G, Waterfield MD. Phosphoinositide 3-kinases: a conserved family of signal transducers. Trends Biochem Sci. 1997;22: 267–72.
7. Curran E, Smith SM. Phosphoinositide 3-kinase inhibitors in lymphoma. Curr Opin Oncol. 2014;26:469–75.
8. Flanagan JU, Shepherd PR. Structure, function and inhibition of the phosphoinositide 3-kinase p110alpha enzyme. Biochem Soc Trans. 2014;42:120–4.
9. Yuan TL, Cantley LC. PI3K pathway alterations in cancer: variations on a theme. Oncogene. 2008;27:5497–510.
10. Huang CH, Mandelker D, Schmidt-Kittler O, Samuels Y, Velculescu VE, Kinzler KW, et al. The structure of a human p110alpha/p85alpha complex elucidates the effects of oncogenic PI3Kalpha mutations. Science. 2007;318:1744–8.
11. Vanhaesebroeck B, Guillermet-Guibert J, Graupera M, Bilanges B. The emerging mechanisms of isoform-specific PI3K signalling. Nat Rev Mol Cell Biol. 2010;11: 329–41.
12. Samuels Y, Wang Z, Bardelli A, Silliman N, Ptak J, Szabo S, et al. High frequency of mutations of the PIK3CA gene in human cancers. Science. 2004;304:554.
13. Burke JE, Perisic O, Masson GR, Vadas O, Williams RL. Oncogenic mutations mimic and enhance dynamic events in the natural activation of phosphoinositide 3-kinase p110alpha (PIK3CA). Proc Natl Acad Sci USA. 2012;109:15259–64.
14. Zhao L, Vogt PK. Helical domain and kinase domain mutations in p110alpha of phosphatidylinositol 3-kinase induce gain of function by different mechanisms. Proc Natl Acad Sci USA. 2008;105:2652–7.
15. Hon WC, Berndt A, Williams RL. Regulation of lipid binding underlies the activation mechanism of class IA PI3-kinases. Oncogene. 2012;31:3655–66.
16. Mandelker D, Gabelli SB, Schmidt-Kittler O, Zhu J, Cheong I, Huang CH, et al. A frequent kinase domain mutation that changes the interaction between PI3Kalpha and the membrane. Proc Natl Acad Sci USA. 2009;106:16996–7001.
17. Chaussade C, Cho K, Mawson C, Rewcastle G, Shepherd P. Functional differences between two classes of oncogenic mutation in the PIK3CA gene. Biochem Biophys Res Commun. 2009;381:577–81.
18. Chaussade C, Rewcastle GW, Kendall JD, Denny WA, Cho K, Gronning LM, et al. Evidence for functional redundancy of class IA PI3K isoforms in insulin signalling. Biochem J. 2007;404:449–58.
19. Costa C, Ebi H, Martini M, Beausoleil SA, Faber AC, Jakubik CT, et al. Measurement of PIP3 levels reveals an unexpected role for p110beta in early adaptive responses to p110alpha-specific inhibitors in luminal breast cancer. Cancer Cell. 2015;27:97–108.
20. Elkabets M, Vora S, Juric D, Morse N, Mino-Kenudson M, Muranen T, et al. mTORC1 inhibition is required for sensitivity to PI3K p110alpha inhibitors in PIK3CA-mutant breast cancer. Sci Transl Med. 2013;5:196ra99.
21. Jamieson S, Flanagan JU, Kolekar S, Buchanan C, Kendall JD, Lee WJ, et al. A drug targeting only p110alpha can block phosphoinositide 3-kinase signalling and tumour growth in certain cell types. Biochem J. 2011;438:53–62.
22. Knight SD, Adams ND, Burgess JL, Chaudhari AM, Darcy MG, Donatelli CA, et al. Discovery of GSK2126458, a highly potent inhibitor of PI3K and the mammalian target of rapamycin. ACS Med Chem Lett. 2010;1:39–43.
23. Furet P, Guagnano V, Fairhurst RA, Imbach-Weese P, Bruce I, Knapp M, et al. Discovery of NVP-BYL719 a potent and selective phosphatidylinositol-3 kinase alpha inhibitor selected for clinical evaluation. Bioorg Med Chem Lett. 2013;23: 3741–8.
24. Gong GQ, Kendall JD, Dickson JMJ, Rewcastle GW, Buchanan CM, Denny WA, et al. Combining properties of different classes of PI3Kalpha inhibitors to

25. understand the molecular features that confer selectivity. Biochem J. 2017;474: 2261–76.
26. Zheng Z, Amran SI, Zhu J, Schmidt-Kittler O, Kinzler KW, Vogelstein B, et al. Definition of the binding mode of a new class of phosphoinositide 3-kinase alpha-selective inhibitors using in vitro mutagenesis of non-conserved amino acids and kinetic analysis. Biochem J. 2012;444:529–35.
27. Fairhurst RA, Gerspacher M, Imbach-Weese P, Mah R, Caravatti G, Furet P, et al. Identification and optimisation of 4,5-dihydrobenzo[1,2-d:3,4-d]bisthiazole and 4,5-dihydrothiazolo[4,5-h]quinazoline series of selective phosphatidylinositol-3 kinase alpha inhibitors. Bioorg Med Chem Lett. 2015;25:3575–81.
28. Fairhurst RA, Imbach-Weese P, Gerspacher M, Caravatti G, Furet P, Zoller T, et al. Identification and optimisation of a 4',5-bisthiazole series of selective phosphatidylinositol-3 kinase alpha inhibitors. Bioorg Med Chem Lett. 2015;25: 3569–74.
29. Gerspacher M, Fairhurst RA, Mah R, Roehn-Carnemolla E, Furet P, Fritsch C, et al. Discovery of a novel tricyclic 4H-thiazolo[5',4':4,5]pyrano[2,3-c]pyridine-2-amino scaffold and its application in a PI3Kα inhibitor with high PI3K isoform selectivity and potent cellular activity. Bioorg Med Chem Lett. 2015;25:3582–4.
30. Hayakawa M, Kawaguchi K, Kaizawa H, Koizumi T, Ohishi T, Yamano M, et al. Synthesis and biological evaluation of sulfonylhydrazone-substituted imidazo [1,2-a]pyridines as novel PI3 kinase p110alpha inhibitors. Bioorg Med Chem. 2007;15:5837–44.
31. Kendall JD, Giddens AC, Tsang KY, Frederick R, Marshall ES, Singh R, et al. Novel pyrazolo[1,5-a]pyridines as p110alpha-selective PI3 kinase inhibitors: exploring the benzenesulfonohydrazide SAR. Bioorg Med Chem. 2012;20:58–68.
32. Bruce I, Akhlaq M, Bloomfield GC, Budd E, Cox B, Cuenoud B, et al. Development of isoform selective PI3-kinase inhibitors as pharmacological tools for elucidating the PI3K pathway. Bioorg Med Chem Lett. 2012;22:5445–50.
33. Heffron TP, Heald RA, Ndubaku C, Wei B, Augistin M, Do S, et al. The Rational design of selective benzoxazepin inhibitors of the alpha-Isoform of phosphoinositide 3-kinase culminating in the identification of (S)-2-((2-(1-isopropyl-1H-1,2,4-triazol-5-yl)-5,6-dihydrobenzo[f]imidazo[1,2-d][1,4]oxazepin-9-yl)oxy)propanamide (GDC-0326). J Med Chem. 2016;59:985–1002.
34. Nacht M, Qiao L, Sheets MP, St Martin T, Labenski M, Mazdiyasni H, et al. Discovery of a potent and isoform-selective targeted covalent inhibitor of the lipid kinase PI3Kalpha. J Med Chem. 2013;56:712–21.
35. Janku F, Tsimberidou AM, Garrido-Laguna I, Wang X, Luthra R, Hong DS, et al. PIK3CA mutations in patients with advanced cancers treated with PI3K/AKT/mTOR axis inhibitors. Mol Cancer Ther. 2011;10:558–65.
36. Luo J, Sobkiw CL, Hirshman MF, Logsdon MN, Li TQ, Goodyear LJ, et al. Loss of class IA PI3K signaling in muscle leads to impaired muscle growth, insulin response, and hyperlipidemia. Cell Metab. 2006;3:355–66.
37. Taniguchi CM, Kondo T, Sajan M, Luo J, Bronson R, Asano T, et al. Divergent regulation of hepatic glucose and lipid metabolism by phosphoinositide 3-kinase via Akt and PKCλ/ζ. Cell Metab. 2006;3:343–53.
38. Irwin JJ, Shoichet BK. Docking screens for novel ligands conferring new biology. J Med Chem. 2016;59:4103–20.
39. Kitchen DB, Decornez H, Furr JR, Bajorath J. Docking and scoring in virtual screening for drug discovery: methods and applications. Nat Rev Drug Discov. 2004;3:935–49.
40. Verdonk ML, Giangreco I, Hall RJ, Korb O, Mortenson PN, Murray CW. Docking performance of fragments and druglike compounds. J Med Chem. 2011;54: 5422–31.
41. Dickson JM, Lee WJ, Shepherd PR, Buchanan CM. Enzyme activity effects of N-terminal His-tag attached to catalytic sub-unit of phosphoinositide-3-kinase. Biosci Rep. 2013;33:e00079.
42. Jones G, Willett P, Glen R, Leach A, Taylor R. Development and validation of a genetic algorithm for flexible docking. J Mol Biol. 1997;267:727–48.
43. Kendall JD, O'Connor PD, Marshall AJ, Frederick R, Marshall ES, Lill CL, et al. Discovery of pyrazolo[1,5-a]pyridines as p110alpha-selective PI3 kinase inhibitors. Bioorg Med Chem. 2012;20:69–85.
44. Gkeka P, Papafotika A, Christoforidis S, Cournia Z. Exploring a non-ATP pocket for potential allosteric modulation of PI3Kalpha. J Phys Chem B. 2015;119:1002–16.
45. Baell JB, Holloway GA. New substructure filters for removal of pan assay interference compounds (PAINS) from screening libraries and for their exclusion in bioassays. J Med Chem. 2010;53:2719–40.
46. Giordanetto F, Kull B, Dellsén A. Discovery of novel class 1 phosphatidylinositide 3-kinases (PI3K) fragment inhibitors through structure-based virtual screening. Bioorg Med Chem Lett. 2011;21:829–35.
47. Yang L, Li G, Ma S, Zou C, Zhou S, Sun Q, et al. Structure–activity relationship studies of pyrazolo[3,4-d]pyrimidine derivatives leading to the discovery of a novel multikinase inhibitor that potently inhibits FLT3 and VEGFR2 and evaluation of its activity against acute myeloid leukemia in vitro and in vivo. J Med Chem. 2013;56:1641–55.